Modelled glacier dynamics over the last quarter of a century at Jakobshavn Isbræ

Ioana S. Muresan[1], Shfaqat A. Khan[1], Andy Aschwanden[2], Constantine Khroulev[2], Tonie Van Dam[3], Jonathan Bamber[4], Michiel R. van den Broeke[5], Bert Wouters[4,5], Peter Kuipers Munneke[5], and Kurt H. Kjær[6]

[1]{Department of Geodesy, DTU Space, Technical University of Denmark, Kgs. Lyngby, Denmark}

[2]{Geophysical Institute, University of Alaska Fairbanks, Fairbanks, Alaska, USA}

[3]{University of Luxembourg, Faculty of Science, Technology and Communication (FSTC), Engineering Research Unit, Luxembourg}

[4]{University of Bristol, School of Geographical Sciences, Bristol, England}

[5]{Institute for Marine and Atmospheric research Utrecht (IMAU), Utrecht University, The Netherlands}

[6]{Centre for GeoGenetics, Natural History Museum of Denmark, University of Copenhagen, Copenhagen, Denmark}

Correspondence to: I. S. Muresan (iomur@space.dtu.dk)

Abstract

Observations over the past two decades show substantial ice loss associated with the speedup of marine terminating glaciers in Greenland. Here we use a regional 3-D outlet glacier model to simulate the behaviour of Jakobshavn Isbræ (JI) located in west Greenland. Our approach represents an attempt to model and understand the recent behaviour of JI with a physical process-based model. Using atmospheric and oceanic forcing we tune our model to reproduce observed frontal changes of JI during 1990–2014. We find that most of the JI retreat during 1990-2014 is driven by ocean forcing and bed geometry. Our results suggest that the overall

variability in modelled horizontal velocities is a response to variations in terminus position. We identify two major accelerations that are consistent with observations of changes in glacier terminus. The first event occurred in 1998, and was triggered by a retreat of the front and moderate thinning of JI prior to 1998. The second event, which started in 2003 and peaked in the summer 2004, was triggered by the final breakup of the floating tongue. This breakup reduced the buttressing at the JI terminus that resulted in further thinning. And as the slope steepened inland over the last decade, sustained high velocities have been observed at JI. Our model provides evidence that the 1998 and 2003 flow accelerations are most likely initiated by the bed geometry. However, our model is not able to capture the observed 2010-2012 terminus retreat. We attribute this slight failing to either inaccuracies in basal topography, or to misrepresentations of the climatic and oceanic forcings that were applied. Both modelled and observed results suggest that JI has been losing mass at an accelerated rate, and that JI continued to accelerate throughout 2014.

1 Introduction

The rate of ice mass loss from Greenland's marine terminating glaciers has more than doubled over the past two decades (Rignot et al., 2008; Moon et al., 2012, Shepherd et al., 2012). Jakobshavn Isbræ, located mid-way up on the west side of Greenland, is one of the largest outlet glaciers in terms of drainage area as it drains ~6 % of the Greenland Ice Sheet (GrIS) (Krabill et al., 2000). Due to its consistently high ice flow rate and seasonally varying flow speed and front position, the glacier has received much attention over the last two decades (Thomas et al., 2003; Luckman and Murray, 2005; Holland et al., 2008; Amundson et al., 2010; Khan et al., 2010; Motyka et al., 2011; Joughin et al., 2012; Gladish et al., 2015a; Gladish et al., 2015b). Measurements from synthetic aperture radar suggest that the ice flow speed of JI doubled between 1992 and 2003 (Joughin et al., 2008). More recent measurements show a steady increase in the flow rate over the glacier's faster-moving region of ~ 5% per year (Joughin et al., 2008). The speedup coincides with thinning of up to 15 m a^{-1} between 2003 and 2012 near the glacier front (Krabill et al., 2004; Nielsen et al., 2013) as observed from airborne laser altimeter surveys. The steady increase in the flow rate and glacier thinning suggest a continuous dynamic drawdown of mass, and they highlight JIs importance for the GrIS mass balance.

Over the past decade, we have seen significant improvements in the numerical modelling of glaciers and ice sheets (e.g. Price et al., 2011; Vieli and Nick, 2011; Winkelmann et al., 2011; Larour et al., 2012; Pattyn et al., 2012; Seroussi et al., 2012; Aschwanden et al., 2013; Nick et al., 2013; Mengel and Levermann, 2014). Some of these models include regional scale glacier models that are based on a flow-line approach (Nick et al., 2009; Parizek and Walker, 2010), and which model the one- or two-dimensional dynamic behaviour of the glacier considered. Flow-line models are computationally efficient and are valuable for understanding the basic processes. However, three-dimensional models are more appropriate in areas of flow divergence/convergence and/or where lateral stresses are important.

In the last decade, several processes have been identified as controlling the observed speedup of JI (Nick et al., 2009; Van der Veen et al., 2011; Joughin et al., 2012). One processes is a reduction in resistance (buttressing) at the marine front through thinning or retreat of the floating tongue of the glacier. But the details of the processes triggering and controlling thinning and retreat remain elusive. Accurately modelling complex interactions between thinning, retreat, and acceleration of flow speed as observed at JI, is challenging. Our knowledge of the mechanisms triggering these events is usually constrained to the period covered by observations. The initial speedup of JI occurred at a time when the satellite and airborne observations were infrequent and therefore insufficient to monitor the annual to seasonal evolution of glacier geometry and speed.

Here, we use a high-resolution, three-dimensional, time-dependent regional outlet glacier model that has been developed as part of the Parallel Ice Sheet Model (PISM; please refer to Sect. 2.1 The ice sheet model) (The PISM Authors, 2014) to investigate the dynamic evolution of JI between 1990 and 2014. While previous 3-D modelling studies have mostly concentrated on modelling individual processes using stress perturbations (e.g. Van der Veen et al., 2011, Joughin et al. 2012), the present aims to model and understand the recent behaviour of JI with a process-based model. Our modelling approach is based on a regional equilibrium simulation and a time-integration over the period 1990 to 2014, where the grounding lines and the calving fronts are free to evolve under monthly climatic forcing and oceanic boundary conditions.

2 Methods and forcing

2.1 The ice sheet model

The ice sheet model used in this study is PISM (stable version 0.6). PISM is an open source, parallel, three-dimensional, thermodynamically coupled and time dependent ice sheet model (Bueler and Brown, 2009; Winkelmann et al., 2011; The PISM Authors, 2014). The ice dynamic model is the "SIA+SSA hybrid", with the non-sliding shallow ice approximation (SIA) for simulating slowly moving grounded ice in the interior part of the ice sheet. For simulating fast-flowing outlet glacier and ice shelf systems (Bueler and Brown, 2009) we use the shallow shelf approximation (SSA). The superposition of SIA and SSA sustains a smooth transition between non-sliding, bedrock frozen ice and sliding, fast-flowing ice, and has been shown to reasonably simulate the flow of both grounded and floating ice (Winkelmann et al., 2011). For conservation of energy, PISM uses an enthalpy scheme (Aschwanden et al., 2012) that accounts for changes in temperature in cold ice (i.e., ice below the pressure melting point) and for changes in water content in temperate ice (i.e., ice at the pressure melting point).

2.1.1 Input data

We use the bed topography from Bamber et al. (2013). The 1 km bed elevation dataset for all of Greenland was derived from a combination of multiple airborne ice thickness surveys and satellite-derived elevations during 1970–2012 (see Supplementary information (SI), Sect. 1.3.2). The terminus position and surface elevation in the Jakobshavn region are based on 1985 aerial photographs and existing satellite altimetry observations (Csatho et al., 2008). Ice thickness in the JI basin is computed as the difference between surface and bedrock elevation, which implies that at the beginning of our equilibrium simulation JI's terminus is considered to be grounded. The model of the geothermal flux is adopted from Shapiro and Ritzwoller (2004). We use input fields of near-surface air temperature and surface mass balance (SMB) from the regional climate model RACMO2.3 (Noël et al., 2015) (see SI, Figs S2 and S3). The version used in this study is produced at a spatial resolution of ~ 11 km and covers the period from 1958 to 2014. The original dataset of 11 km grid is interpolated to 2 x 2 km grids using bilinear interpolation.

2.1.2 Boundary conditions, calving and ground line parametrization

In our model, the three-dimensional ice enthalpy field, basal melt, modelled amount of till-pore water, and lithospheric temperature are obtained from an ice-sheet-wide paleo-climatic spin-up. The paleo-climatic spin-up follows the initialization procedure described by Bindschadler et al. (2013) and Aschwanden et al. (2013). We start the spin-up on a 10 km grid, and then we refine to 5 km at -5ka. It is important to note that during the paleo-climatic initialization the terminus is held fixed to the observed 1990 position in the JI region, and to the present-day position elsewhere.

In the regional outlet glacier model of PISM, the boundary conditions are handled in a 10 km strip positioned outside of the JI's drainage basin and around the edge of the computational domain. In this strip, the input values of the basal melt, the amount of till-pore water, ice enthalpy, and lithospheric temperature (Aschwanden et al., 2013) are held fixed and applied as Dirichlet boundary conditions in the conservation of energy model (The PISM Authors, 2014). Along the ice shelf calving front, we apply a physically based calving (eigencalving) parametrization (Winkelmann et al., 2011; Levermann et al., 2012) and an ice thickness condition (Albrecht et al., 2011) that removes at a rate of at most one grid cell per time step, any floating ice at the calving front thinner than a given threshold (see SI Sect. 1, Table S2 for its specific value). The average calving rate (c) is calculated as the product of the principal components of the horizontal strain rates ($\dot{\varepsilon}_{\pm}$), derived from SSA velocities, and a proportionality constant parameter (k) that captures the material properties relevant for calving :

$$c = k\dot{\varepsilon}_{+}\dot{\varepsilon}_{-} \quad \text{for } \dot{\varepsilon}_{\pm} > 0. \qquad (1)$$

The strain rate pattern is strongly influenced by the geometry and the boundary conditions at the ice shelf front (Levermann et al. (2012)). A partially-filled grid cell formulation (Albrecht et al., 2011), which allows for sub-grid scale retreat and advance of the front is used to connect the calving rate computed by the eigen calving parametrization with the mass transport scheme at the ice shelf terminus. The calving law is known to yield realistic calving front positions for various types of ice shelves being successfully used for modelling calving front positions in whole Antarctica simulations (Martin et al., 2011) and regional east Antarctica simulations (Mengel and Levermann, 2014).

The parameterization of the grounding line position is based on the "LI" parameterization (Gladstone et al., 2010) and is not subject to any boundary conditions. At each time step the grounding line position is determined by a mask which distinguishes between grounded and floating ice using a flotation criterion based on the modelled ice thickness (Winkelmann et al., 2011):

$$b(x,y) = -\frac{\rho_i}{\rho_o} H(x,y) \qquad (2)$$

where (x,y) give the horizontal dimension, ρ_i is the density of the ice, ρ_o is the density of the ocean water and H represents the ice thickness. Therefore, the grounding line migration is influenced by the ice thickness evolution, which further depends on the velocities computed from the stress balance. The superposition of SIA and SSA, which implies that the SSA velocities are computed simultaneously for the shelf and for the sheet, ensures that the stress transmission across the grounding line is continuous and that buttressing effects are included. In the Mismip3d experiments, PISM was used to model reversible grounding line dynamics with results consistent with full-Stokes models (Feldmann et al., 2014). However, we have not performed the Mismip3d experiments for our particular parameter settings and therefore, the accuracy of the modelled grounding line migration is solely based on the results presented in Feldmann et al. (2014).

We start our regional JI runs with an equilibrium simulation on a 125 × 86 horizontal grid with 5 km spacing and a vertical resolution of 20 m. The enthalpy formulation models the mass and energy balance for the three-dimensional ice fluid field based on 200 regularly spaced layers within the ice. The temperature of the bedrock thermal layer is computed up to a depth of 1000 m with 50 regularly spaced layers. The first step is to obtain a 5 km regional equilibrium model for JI using constant mean climate (i.e. repeating the 1960-1990 mean air temperature and surface mass balance; see 2.1.1 Input data). We consider that equilibrium has been established when the ice volume in the regional domain changes by less than 1% in the final 100 model years. Grid refinements are made from 5 km (125×86) to 2 km (310×213) after 3000 years. The length of the simulation with the 2 km grid is 200 years. The model reaches equilibrium with an ice volume of $0.25 \cdot 10^6$ km^3 (or a 3.6 % increase relative to the input dataset from Bamber et al. (2013) adjusted to simulate, 1990's metrics; see Sect. 2.1.1). Further, using our equilibrium simulations with a 2 km horizontal grid and a 10 m vertical grid, we integrate forward in time (hindcast) from 1990 to 2014 by imposing monthly fields of SMB and 2 m air temperatures through a one-way coupling scheme. The calving fronts and

grounding lines are free to evolve in time both during the regional equilibrium and the forward simulation.

2.1.3 Parameterization for ice shelf melting

We use a simple parametrization for ice shelf melting where the melting effect of the ocean is based on both sub-shelf ocean temperature and salinity (Martin et al., 2011). At the base of the ice shelf, the sub-shelf ice temperature (T_{pm}) is set to the pressure-melting temperature and is applied as a Dirichlet boundary condition in the conservation of energy equation. The sub-shelf ice temperature holds the following form:

$$T_{pm} = 273.15 + \beta_{cc} z_b \qquad (3)$$

where $\beta_{cc} = 8.66 \times 10^{-4}$ K m^{-1} represents the Clausius-Clapeyron gradient and z_b represents the elevation at the base of the ice shelf.

The sub-shelf mass flux is used as a source in the mass-continuity equation. This mass flux from shelf to ocean (S) follows Beckmann and Goosse (2003) and is computed as a heat flux (Q_{heat}) between the ocean and ice that represents the melting effect of the ocean through both temperature and salinity (Martin et al., 2011):

$$S = \frac{Q_{heat}}{L_i \rho_i} \qquad (4)$$

$$Q_{heat} = \rho_o c_{p_o} \gamma_T F_{melt} (T_o - T_f) \qquad (5)$$

where $L_i = 3.35 \times 10^5$ J kg^{-1} is the latent heat capacity of ice, $c_{p_o} = 3974$ J (kg K)$^{-1}$ is the specific heat capacity of the ocean mixed layer, $\gamma_T = 10^{-4}$ m s^{-1} is the thermal exchange velocity, F_{melt} is a model parameter (see SI, Table S2), T_o is the ocean water temperature and T_f is the virtual temperature. This virtual temperature represents the freezing temperature of ocean water at the depth z_b below the ice shelf and has the form:

$$T_f = 273.15 + 0.0939 - 0.057 S_o + 7.64 \times 10^{-4} z_b \qquad (6)$$

where S_o is the salinity of the ocean.

We start our simulations with a constant ocean water temperature (T_o) of -1.7 °C, which is further scaled by the ice shelf melting parametrization spatially and temporally based on the depth below the ice shelf (geometry) and the ocean water salinity (see also SI, Fig. S4). Therefore, the sub-shelf melt rates are dependent on the ice shelf thickness and indirectly to

the bed topography depth. We choose to keep the ocean water salinity ($S_o = 35$ psu) constant in time and space as the model does not capture the salinity gradient from the base of the ice shelf through layers of low and high salinity. However, a previous study conducted by Mengel and Levermann (2014) using the same model established that the sensitivity of the melt rate to salinity is negligible.

3 Results and discussion

We perform fifty simulations with different sets of parameters. The parameters are altered only during the regional JI runs. From these results, we present here the parameterization that best captures the full evolution of JI during the period 1990–2014 (see SI, Sect. 1.1 for the values of the ice sheet model parameters). The sensitivity to parameters controlling ice dynamics, basal processes, ice shelf melt and ocean temperature are discussed in SI, Sect. 1.2. The evolution of the main driver variables for the atmosphere and the ocean are further described in SI, Sect. 1.2.5.

We calibrated the parameters such that the model reproduces the frontal positions (Fig. 2) and the ice mass change observations (Fig. 4, please refer to Sect. 3.1.2 Ice mass change) at JI during the period 1990-2014 and 1997-2014, respectively.

3.1 Observations vs. modelling results

3.1.1. Annual scale variations in velocities, terminus and grounding line positions

We investigate the processes driving the dynamic evolution of JI and its variation in velocity between 1990–2014 with a focus on the initial speedup of JI and the 2003 breakup of the ice tongue. The overall pattern observed in our simulations suggests a gradual increase in velocities that agrees well with observations (Joughin et al., 2014) (Fig. 3). Three distinct stages of acceleration are identified in Fig. 3 (see also Movie 1) and discussed in detail below.

- **1990–1997**

  The first speedup is caused by a retreat of the front position by approximately 2 to 4 km between 1990 and 1991. There is no observational evidence that this retreat actually occurred. It is probably a modelling artefact as the geometry obtained during the regional equilibrium simulation is forced with new oceanic and atmospheric conditions. This acceleration (Fig. 3) is caused by a reduction in

buttressing due to a reduction in lateral resistance (Van der Veen et al., 2011), which is generated by the gradual retreat of the front, and which triggers a dynamic response in the upstream region of JI.

Starting in 1992 we obtain a good fit between modelled and observed frontal positions. Disregarding the acceleration in 1991–1992, no significant seasonal fluctuation in flow rate is modelled during this period. These results are consistent with observations (Echelmeyer et al., 1994). From 1993 a stronger seasonal velocity signal begins to emerge in our simulation that continues and intensifies in magnitude during 1994 and 1995. The departure in 1995 from the normal seasonal invariance in velocity seems to be in our model influenced by the climate forcing (see SI, Figs. S2, S9, and S12(A, B)). This indicates that, as suggested by Luckman and Murray (2005), the 1995 anomalously high melt year (see Figs. S2 and S3) may have potentially contributed to JIs retreat and flow acceleration during this period. The modelled velocities for 1992 and 1995 are consistent with observed velocities for the same period (Joughin et al., 2008; Vieli et al., 2011). In 1996 and 1997, the frontal extent and the grounding line position remain relatively stable (Figs. 2 and 6), and no significant seasonal fluctuation in ice flow rate is modelled. These model results agree well with observations, which indicate that the glacier speed was relatively constant during this period (Luckman and Murray, 2005).

- **1998–2002**

According to observations (Joughin et al., 2004; Luckman and Murray, 2005; Motyka et al., 2011; Bevan et al., 2012), the initial acceleration of JI occurred in May-August 1998, which coincides with our modelled results. In our simulation, the 1998 acceleration is generated by a retreat of the terminus in 1997-1998, which may be responsible for reduction in buttressing (see Movie 1 and SI, Fig. S7). Thinning, both near the terminus and inland (up to 10 km away from the 1990 front position), starts in our model in the summer of 1995 and continues to accelerate after 1998 (Figs. 3 and 6). These findings are corroborated both by observations (SI, Fig. S15) and modelling results (Fig. 3). Although thinning appears to have increased in our model during three continuous years we find little additional speedup during the period prior to 1998 (Figs. 2, 6, and S7). According to our simulation, JI's speed increased in the summer of 1998 by ~ 80% relative to the

summer of 1992 (Fig. 3). Our model suggests a retreat of the grounding line position starting in 1998 that accelerates thereafter (Figs. 2, 6, and S7). The period between 1999 and 2002 is in our simulation characterized by a temporal uniform flow, with no episodes of significant terminus retreat. Overall modelling results suggest an advance of the terminus between 1999 and 2000 and a retreat of the southern tributary between 2000 and 2002 by ~4 km, which correlates with existing observations (Thomas, 2004). Concurrent with the 1998-2001 terminus retreat, the grounding line retreats in our model by ~6 km (Figs. 2 and 6). Calving and thinning near the front continuous in 2002 and results in decrease in resistive stresses at the terminus (see SI, Figs. S7 and S8).

- **2003–2014**

In the late summer of 2003, an increase in flow velocity is observed (Fig. 3), which is driven in our simulations by the final breakup of the ice tongue (see Figs. 2 and 6). The period, 2002-2003, is characterized by substantial retreat of the front (~4-6 km) and the grounding line (~4 km), which starts in June 2002 and continues throughout 2003. By December 2003 the terminus has retreated back to the position of the grounding line (see Figs. 2 and 6). The retreat that occurred in 2003 and the loss of the floating tongue caused a major decrease in resistive stresses near the terminus (see SI, Figs. S7 and S8). By 2004 the glacier has thinned significantly, both near the front, and further inland in response to a change in the near-terminus stress field (Figs. 3 and 6). During the final breakup of the ice tongue, JI reached unprecedented flow rates, which in our simulation are as high as 20 km a^{-1} (~ 120% increase relative to 1998). The velocities decreased to 16 km a^{-1} (~ 80% increase relative to 1998) in the subsequent months, and JI remains relatively stable with high seasonal fluctuations. The high velocities observed at JI after the loss of its floating tongue are further sustained in our simulation by the thinning that occurred in 2004 onward (see Fig. 3), which continues to steepen the slopes near the terminus (see Fig. 6), and by a seasonal driven (sub-annual scale) retreat and advance of the front. This thinning is combined in the following years with a reduction in surface mass balance due to increased melting and runoff (van den Broeke et al., 2009; Enderlin et al., 2014, Khan et al., 2014). The period 2004-2014 is characterized in our simulation by relatively uniform velocity peaks with strong seasonal variations (Fig. 3). During this

period, the terminus remained close to the grounding line with no episodes of significant retreat.

In agreement with previous studies (e.g. Joughin et al. 2012), our results suggest that the overall variability in the modelled horizontal velocities is a response to variations in terminus position (see SI, Fig. S7 and Sect. 1.4 for more details). The terminus retreat is mostly driven in our model by the sub-shelf melting parametrization applied (see SI, Sect. 1.2.5 and Figs. S5, S12). In terms of seasonality, our results suggest that most of the seasonal signal in the model is climate driven (see SI, Sect. 1.4 and Fig. S12).

3.1.2 Ice mass change

Figure 4 shows observed and modelled mass change for the period 1997 to 2014. We estimate the rate of ice volume change from airborne and satellite altimetry over the same period and convert to mass change rate (see SI, Sect. 2 for more details). Overall there is good agreement between modelled and observed mass change (see Fig. 4), and our results are in agreement with other similar studies (Howat et al., 2011; Nick et al., 2013). Dynamically driven discharge is known to control Jakobshavn's mass loss (Nick et al., 2013). The modelled cumulative mass loss is 269 Gt, of which 93% (~251 Gt) is determined to be dynamic in origin while the remaining 7% (~18 Gt) is attributed to a decrease in SMB (see Fig. 4). Further, the present-day unloading of ice causes the Earth to respond elastically. Thus, we can use modelled mass changes to predict elastic uplift. We compare modelled changes of the Earth's elastic response to changes in ice mass to uplift observed at four GPS sites (see Fig. 5 and SI, Sect. 3). Both model and observations consistently suggest large uplift near the JI front and somewhat minor uplift rates of few mm a^{-1} at distances of >100km from the ice margin.

Although the terminus has ceased to retreat in our simulations after 2009 (see Fig. 6 and SI, Fig. S7), the mass loss, and most important the dynamic mass loss, has continued to accelerate (see Fig. 4). Our results show (SI, Figs. S7 and S8) that during this period the mass change is mostly driven by the sub-annual terminus retreat and advance, which continues to generate dynamic changes at JI through seasonal (sub-annual scale) reductions in resistive stresses.

3.2 Feedback mechanisms, forcings and limitations

Representing the processes that act at the marine boundary (i.e. calving and ocean melt) are significantly important for understanding and modelling the retreat/advance of marine terminating glaciers like JI. Determining terminus positions by using a physical based calving law with horizontal strain rates (see Sect. 2.1.2) is motivated by the model's ability to maintain realistic calving front positions (Levermann et al., 2012). Although, the calving law was designed and primarily used for modelling large ice shelves specific to the Antarctic ice sheet, our results show that the calving law also performs well for the narrow, deep fjords characterized by JI (see Fig. 2). The benefit of using such a calving law is that it can evolve the terminus position with time and thus, potential calving feedbacks are not ignored. As the terminus retreats, the feedback between calving and retreat generates dynamic changes due to a reduction in lateral shear and resistive stresses (see SI, Figs. S7 and S8). In a simulation in which the terminus position is kept fixed to the 1990s position, the velocity peaks are uniform (i.e. no acceleration is modelled except for some seasonal related fluctuations generated by the climatic forcing applied) and the mass loss remains relatively small (~ 70 Gt). Therefore, consistent with Vieli et al. (2011), we find that this feedback between calving and retreat is highly important in modelling JI's dynamics.

As introduced in Sect. 2.1.2, our approach here is to adjust the terminus in the JI region to simulate the 1990s observed front position and surface elevation based on aerial photographs and available satellite altimetry observations (Csatho et al., 2008). The glacier terminus in 1990s is known to have been floating (Csatho et al., 2008; Motyka et al. 2011), but details regarding its thickness are not known. Motyka et al. (2011) calculated the 1985 hydrostatic equilibrium thickness of the south branch floating tongue from smoothed surface DEMs and obtained a height of 600 m near the calving front and 940 m near the grounding zone. In this paper however, we choose to use a more simplistic approach in which we compute the thickness as the difference between the surface elevation and the bed. This implies that our simulations start with a grounded terminus. The geometry of the terminus plays an important role in parameterizing ice shelf melting, and therefore our choice could directly affect the magnitude of the basal melt rates (see SI, Sect. 1.2.8). As expected, the difference in geometry results in modelled basal melt rates slightly larger than those obtained by Motyka et al. (2011). As shown in Fig. 6, the glacier starts to develop a large floating tongue in 1999 and

the model is able to simulate with much accuracy its breakup that occurred in late summer 2003 and the subsequent glacier acceleration.

Starting in 2010 the retreat of the terminus did not correlate well with observations (see Fig. 2). The terminus and the grounding line retreat does not cease after 2010. Further, observed front positions (Joughin et al., 2014) suggests that by summer 2010 JI was already retreating over the sill and on the overdeepning indicated by the red star in Fig. 6. The observed retreat is not reproduced in our simulations (see Fig. 6) suggesting that additional feedbacks and/or forcings must continue to disturb the glacier. These feedbacks may not be well represented (e.g. missing physics, inaccuracies in climatic or oceanic conditions) or simply may not be captured by the model due to various limitations (e.g. bed topography model constraints and grid resolution; see SI, Sect. 1.3 for more details). As detailed in SI, Sect. 1.3.2, the basal topography of JIs channels represents a large source of uncertainty. The terminus retreat is mostly driven in our model by the sub-shelf melting parametrization that we applied (see SI, Fig. S4) that is highly dependent on the bed geometry. In our simulation the grounding line shows stabilization downstream of the sill after 2005 (see Fig. 2 and Fig. 6), which is in accordance with previous modelling studies (Vieli et al., 2001, Vieli et al., 2011). The grounding line behaviour is crucial for the dynamics of marine outlet glaciers, as its migration removes areas of flow resistance at the base and may trigger unstable retreat if the glacier is retreating into deeper waters. Vieli et al. (2011) found that by artificially lowering the same bed sill with 100 m, the grounding line eventually retreats and triggers a catastrophic retreat of 80 km in just over 20 years. Similar to Vieli et al. (2011), the grounding line in our simulation does not manage to retreat upstream over the shallow sill. In an equivalent experiment performed with our model, lowering the bed sill by 100 m, did not result in a retreat of the grounding line over the sill.

From a climatic perspective, the summer of 2012 was characterized by exceptional surface melt, covering 98% of the entire ice sheet surface, including the high elevation Summit region (Nghiem et al., 2012; Hanna et al., 2014). Overall, the 2012 melt-season was two months longer than the 1979–2011 mean and the longest recorded in the satellite era (Tedesco et al., 2013). Furthermore, the summer of 2012 was preceded by a series of warm summers (2007, 2008, 2010 and 2011) (Hanna et al., 2014). Over the average surface melt was already recorded in May-June 2012 (see Fig. 3 from NSIDC (2015)) when most of the 2011-2012 winter accumulation melted and over 30% of the ice sheet surface experienced surface melt.

An intense and long melt year leads to extensive thinning of the ice, and has the potential to enhance hydrofracturing of the calving front due to melt water draining into surface crevasses (MacAyeal et al., 2003; Joughin et al., 2013; Pollard et al., 2015) resulting in greater and/or faster seasonal retreat and an increase in submarine melt at the terminus and the sub-shelf cavity (Schoof, 2007; Stanley et al., 2011; Kimura et al., 2014; Slater et al., 2015). The seasonal retreat of JIs terminus started relatively early in 2012, with a large calving event having already occurred in June. While it seems difficult to attribute this particular calving event solely to processes related with the 2012 melt season, it does seem probable that the series of warm summers (2007-2011) together with the 2012 exceptional melt season could have enhanced hydrofracturing of the calving front and consequently could have induced a retreat of the terminus which cannot be captured by the model (i.e. in its present configuration the model does not account for the influence of meltwater runoff and its role in the subglacial system during surface melt events). In our model, the climatic forcing applied can influence JI's dynamics only through changes in surface mass balance (SMB) (i.e., accumulation and ablation) (see SI, Sect. 1.2.5). Our results suggest that most of the sub-annual signal in the model is climate driven (see SI, Sect. 1.4 and Fig. S12). A comparison between a simulation that includes the full climatic variability (monthly temperature and SMB from RACMO2.3) and a simulation with constant climatic forcing (mean 1960-1990 temperature and SMB) indicates that the two accelerations, in 1998 and 2003, are related to bed geometry and ocean melt. Furthermore, our results show that some seasonal velocity peaks could potentially be influenced by the climatic forcing applied (see Figs. S9 and S12(A,B)). This suggests that even though the climate does not trigger and sustain long accelerations, the climate certainly does have the capacity to contribute and accentuate the processes that are responsible for these accelerations. The modelled sub-annual signal in terms of terminus retreat and velocities does not always correlate with the observed signal, suggesting that potentially different seasonal forcings (e.g. ice mélange variability, seasonal ocean temperature variability) may influence the advance and retreat of the front at seasonal scales. The ice mélange can prevent the ice at the calving front from breaking off and therefore could reduce the calving rates. The introduction of an ice mélange parametrization will probably help to minimize some of the sub-annual noise observed in our simulations (see Fig. 3). Furthermore, the 2 km resolution used in this study may not be sufficient to accurately model the seasonal retreat and advance of the front. The smallest calving event in our model is 4 km^2, which is larger than most of the calving events observed at JI (see SI, Sect. 1.3.1).

Concerning the ocean conditions, warm water temperatures in the fjord were recorded in 2012. Besides a cold anomaly in 2010, which was sustained until early 2011, the period 2008-2013 is characterized by high fjord waters temperatures - equal to or warmer than those recorded in 1998-1999 (Gladish et al., 2015). In our model, the ice melt rates are determine from the given conditions in temperature (-1.7 °C), and salinity (35 psu) of the fjord waters, and the given geometry (see Sect. 2.1.3 and SI, Sect. 1.2.5). Although, the ocean temperature is scaled based on a virtual temperature that depends on the geometry of the shelf, the 1998 and 2003 accelerations can be modelled without additional variability in ocean temperatures. Further our results suggest that these accelerations are most likely driven by internal glacier dynamics and bed geometry, and not by an increase in e.g. ocean temperature. The fact that we are able to model JIs retreat with no variability in ocean temperature suggests that the retreat and acceleration observed at JI are likely not caused by a year to year variability in ocean temperatures. This conclusion agrees with the observational study of Gladish et al. (2015) who analysed ocean temperature variability in the Ilulissat fjord with JI variability and who found that after 1999 there was no clear correlation. Our results do not, however, imply that the ocean influence in JI's retreat is negligible (see Fig. S5), but rather that the glacier most likely responds to changes in ocean temperature that are sustained for longer time periods. Two additional experiments, where the input ocean temperature (T_o) was increased to -1 °C indicate that higher melt rates beneath the grounding line could potentially explain the retreat observed after 2010. In the first experiment, the input T_o was increased from -1.7 °C to -1 °C between 1997-2014 (Gladish et al., 2015). This generated in our simulation, for the period 1997-2014, an accelerated retreat of the front that does not correlate with observations, and mass loss estimates significantly larger (by ~ 50 %) than those calculated from airborne and satellite altimetry observations (see SI, Sect. 2). In the second experiment, T_o was increased to -1 °C between 2010-2014 (with (T_o-T_f) ~ +0.7°C at the base of the shelf in 2010), and generated in our simulation, for the period 2010-2014, a faster retreat of the front that correlates well with observations, and an increase of mass loss by ~7 Gt.

4 Conclusions

In this study, a three-dimensional, time-dependent regional outlet glacier model is used to investigate the processes driving the dynamic evolution of JI and its seasonal variation in ice velocity between 1990 and 2014. Here, we attempt to model and understand the recent

behaviour of JI with a process-based model. The model parameters were calibrated such that the model reproduces observed frontal positions (Fig. 2) and ice mass change observations (Fig. 4) at JI over the periods 1990-2014 and 1997-2014, respectively. We obtain a good agreement of our model output with measured horizontal velocities, observed thickness change, and GPS derived elastic uplift of the crust (Figs. 3 and 5).

Our results suggest that most of the JI retreat during 1990-2014 is ocean and bed geometry driven and that the overall variability in the modelled horizontal velocities is a response to variations in terminus position. The seasonal variability observed in our simulations is climate driven. In its present configuration, the model does not account for seasonal ocean temperature and ice mélange variability that may influence the seasonal advance and retreat of the front.

For the period 1990-2010, the model is able to capture the overall retreat of the terminus and the trends in the observed velocities (see Figs. 2 and 3). The 2010-2012 observed terminus retreat (Joughin et al., 2014) is, however, not reproduced in our simulations, likely due to inaccuracies in basal topography, or misrepresentations of the climatic and oceanic forcings.

Our model provides evidence for two distinct flow accelerations in 1998 and 2003 that are consistent with observations. The first was generated by a retreat of the terminus and moderate thinning prior to 1998; the latter was triggered by the final breakup of the floating tongue. During this period, JI attained unprecedented velocities reaching as high as 20 km a^{-1}. Additionally, the final breakup of the floating tongue generated a reduction in buttressing that resulted in further thinning. Over the last decade, as the slope steepened inland, sustained high flow rates were observed at JI. In accordance with previous studies (Thomas, 2004; Joughin et al., 2012), our findings suggest that the speed observed today at JI is a result of thinning induced changes due to reduction in resistive stress (buttressing) near the terminus correlated with inland steepening slopes (Figs. 6 and S7). Both model and observations suggest that JI has been losing mass at an accelerating rate and that the glacier has continued to accelerate through 2014 (Fig. 4). Similar to previous studies (Nick et al., 2009; Vieli et al., 2011; Joughin et al. 2012), our results show that the dynamic changes observed at JI are triggered at the terminus (SI, Figs. S5 and S6). In our model, the terminus retreat is mostly driven by the sub-shelf melting parametrization applied. Thus, our results suggest that ocean forcing is the principal driver for the retreat observed over the last 2 decades. Further, our model provides evidence that the rapid accelerations of JI in 1998 and 2003 could be triggered by the bed

geometry and internal glacier dynamics, and not by a sudden increase in e.g. ocean temperature.

Author Contributions

I.S.M. was responsible for the numerical modelling part. J.B. provided the bed model. M.R.V.D.B, and P.K.M. provided climate data. S.A.K and B.W. provided observational data. I.S.M. and S.A.K created the figures and wrote the manuscript with contributions from A. A, J.B., T.V.D., M.R.V.D.B, B.W., P.K.M, K.K., and C.K.

Acknowledgements

Ioana S. Muresan is funded by the Forskningsraadet for Natur og Univers (grant no. 12-155118). Shfaqat A. Khan is supported by Carlsbergfondet (grant no. CF14-0145). Jonathan Bamber was part funded by UK NERC grant NE/M000869/1. Bert Wouters is funded by a Marie Curie International Outgoing Fellowship within the 7th European Community Framework Programme (FP7-PEOPLE-2011-IOF-301260). The development of PISM is supported by NASA grants NNX13AM16G and NNX13AK27G. We thank the editor, three anonymous reviewers for their valuable comments and suggestions to improve and clarify the manuscript, and Veit Helm for providing cryosat-2 data.

References

Albrecht, T., M. Martin, M. Haseloff, R. Winkelmann, and A. Levermann. 2011. "Parameterization for subgrid-scale motion of ice-shelf calving fronts." The Cryosphere 5: 35–44. doi:10.5194/tc-5-35-2011.

Amundson, J. M., M. Fahnestock, M. Truffer, J. Brown, M. P. Lüthi, and R. J. Motyka. 2010. "Ice mélange dynamics and implications for terminus stability, Jakobshavn Isbræ, Greenland." Journal of Geophysical Research 115: F01005. doi:10.1029/2009JF001405.

Aschwanden, A., E. Bueler, C. Khroulev, and H. Blatter. 2012. "An enthalpy formulation for glaciers and ice sheets." Journal of Glaciology 58(209): 441–457. doi:10.5194/tcd-6-5069-2012. doi:10.3189/2012JoG11J088.

Aschwanden, A., G. Aðalgeirsdóttir, and C. Khroulev. 2013. "Hindcast to measure ice sheet model sensitivity to initial states." The Cryosphere 7: 1083–1093. doi:10.5194/tcd-6-5069-2012.

Bamber, J. L., J. A. Griggs, R. T. W. L. Hurkmans, J. A. Dowdeswell, S. P. Gogineni, I. Howat, J. Mouginot, J. Paden, S. Palmer, E. Rignot, and D. Steinhage. 2013. "A new bed elevation dataset for Greenland." The Cryosphere 7: 499–510. doi:10.5194/tc-7-499-2013.

Beckmann, A., and H. Goosse. 2003. "A parameterization of ice shelf–ocean interaction for climate models." Ocean Modeling 5 (2): 157–170. doi:10.1016/S1463-5003(02)00019-7.

Bevan, S. L., A. J. Luckman, and T. Murray. 2012. "Glacier dynamics over the last quarter of a century at Helheim, Kangerdlugssuaq and other major Greenland outlet glaciers." The Cryosphere 6: 923–937. doi:10.5194/tc-6-923-2012.

Bindschadler, R. A., S. Nowicki, A. Abe-Ouchi, A. Aschwanden, H. Choi, J. Fastook, G. Granzow, et al. 2013. "Ice-Sheet Model Sensitivities to Environmental Forcing and Their Use in Projecting Future Sea Level (the SeaRISE Project)." Journal of Glaciology 59 (214): 195–224. doi:10.3189/2013JoG12J125.

Broeke, M. van den, J. Bamber, J. Ettema, Eric Rignot, E. Schrama, W. J. van de Berg, E. van Meijgaard, I. Velicogna, and B. Wouters. 2009. "Partitioning recent Greenland mass loss." Science 326 (5955): 984–986. doi:10.1126/science.1178176.

Bueler, E., and J. Brown. 2009. “Shallow shelf approximation as a ‘sliding law’ in a thermodynamically coupled ice sheet model.” Journal of Geophysical Research 114: F03008. doi:10.1029/2008JF001179.

Csatho, B., T. Schenk, C. J. Van Der Veen and W. B. Krabill. 2008. “Intermittent thinning of Jakobshavn Isbræ, West Greenland, since the Little Ice Age.” Journal of Glaciology 54 (184): 131–144. doi: 10.3189/002214308784409035.

Echelmeyer, K.A., W.D. Harrison, C. Larson, and J.E. Mitchell. 1994. The role of the margins in the dynamics of an active ice stream. Journal of Glaciology 40(136): 527–538.

Enderlin, E. M., I. M. Howat, and A. Vieli. 2013. “High sensitivity of tidewater outlet glacier dynamics to shape.” The Cryosphere 7: 1007–1015. doi: 10.5194/tc-7-1007-2013.

Enderlin, E. M., I. M. Howat, S. Jeong, M. J. Noh, J. H. van Angelen, and M. R. van den Broeke. 2014. “An improved mass budget for the Greenland ice sheet.” Geophysical Research Letters 41: 866–872. doi:10.1002/2013GL059010.Feldmann, J., T. Albrecht, C. Khroulev, F. Pattyn, and A. Levermann. 2014. “Resolution-dependent performance of grounding line motion in a shallow model compared with a full-Stokes model according to the MISMIP3d intercomparison.” Journal of Glaciology 60 (220): 353–360. doi:10.3189/2014JoG13J093.

Feldmann, J., Albrecht, T., Khroulev, C., Pattyn, F., and Levermann, A.: Resolution-dependent performance of grounding line motion in a shallow model compared with a full-Stokes model according to the MISMIP3d intercomparison, J. Glaciol., 60, 353–360, doi:10.3189/2014JoG13J093, 2014.

Gladish, C. V., D. M. Holland, and C. M. Lee. 2015a. “Oceanic boundary conditions for Jakobshavn Glacier. Part II: Provenance and sources of variability of Disko Bay and Ilulissat icefjord waters, 1990–2011.” Journal of Physical Oceanography 45: 33–63. doi:dx.doi.org/10.1175/JPO-D-14-0045.1.

Gladish, C. V., D. M. Holland, A. Rosing-Asvid, J. W. Behrens, and J. Boje. 2015b. “Oceanic boundary conditions for Jakobshavn Glacier. Part I: Variability and renewal of Ilulissat icefjord waters, 2001–2014.” Journal of Physical Oceanography 45: 3–32. doi:dx.doi.org/10.1175/JPO-D-14-0044.1.

Gladstone, R. M., A. J. Payne, and S. L. Cornford. 2010. “Parameterising the grounding line in flow-line ice sheet models.” The Cryosphere 4: 605–19. doi:10.5194/tc-4-605-2010.

Hanna, E., X. Fettweis, S. Mernild, J. Cappelen, M. Ribergaard, C. Shuman, K. Steffen, L. Wood, and T. Mote. 2014. "Atmospheric and oceanic climate forcing of the exceptional Greenland ice sheet surface melt in summer 2012." International Journal of Climatology 34 (4): 1022–1037. doi:10.1002/joc.3743.

Holland, D. M., R. H. Thomas, B. de Young, M. H. Ribergaard, and B. Lyberth. 2008. "Acceleration of Jakobshavn Isbræ Triggered by Warm Subsurface Ocean Waters." Nature Geoscience 1: 659–664. doi:10.1038/ngeo316.

Howat I. M., Y. Ahn, I. Joughin, M. R. van den Broeke, J. T. M. Lenaerts, and B. Smith. 2011. "Mass balance of Greenland's three largest outlet glaciers, 2000–2010." Geophysical Research Letters 38(12): L12501. doi: 10.1029/2011GL047565.

IPCC. 2013. "Climate Change 2013: The Physical Science Basis. Contribution of Working Group I to the Fifth Assessment Report of the Intergovernmental Panel on Climate Change." Cambridge University Press, Cambridge, United Kingdom and New York, NY, USA: 1535 pp. doi:10.1017/CBO9781107415324.

Joughin, I., I. M. Howat, M. Fahnestock, B. Smith, W. Krabill, R. B. Alley, H. Stern, and M. Truffer. 2008. "Continued evolution of Jakobshavn Isbrae Following Its Rapid Speedup." Journal of Geophysical Research 113: F04006. doi:10.1029/2008JF001023.

Joughin, I, B. E. Smith, I. M. Howat, T. Scambos, and T. Moon. 2010. "Greenland Flow Variability from Ice-Sheet-Wide Velocity Mapping". Journal of Glaciology 56 (197): 415-430. doi:10.3189/002214310792447734.

Joughin, I., I. Howat, B. Smith, and T. Scambos. 2011. "MEaSUREs Greenland Ice Velocity: Selected Glacier Site Velocity Maps from InSAR". Boulder, Colorado, USA: NASA DAAC at the National Snow and Ice Data Center. doi:10.5067/MEASURES/CRYOSPHERE/nsidc-0481.001.

Joughin, I., B. E. Smith, I. M. Howat, D. Floricioiu, R. B. Alley, M. Truffer, and M. Fahnestock. 2012. "Seasonal to decadal scale variations in the surface velocity of Jakobshavn Isbræ, Greenland: Observation and model-based analysis." Journal of Geophysical Research 117: F02030. doi:10.1029/2011JF002110.

Joughin, I., S. B. Das, G. E. Flowers, M. D. Behn, R. B. Alley, M. A. King, B. E. Smith, J. L. Bamber, M. R. van den Broeke, and J. H. van Angelen. 2013. "Influence of ice-sheet

geometry and supraglacial lakes on seasonal ice-flow variability." The Cryosphere 7: 1185-1192. doi:10.5194/tc-7-1185-2013.

Joughin, I., B. E. Smith, D. E. Shean, and D. Floricioiu. 2014. "Brief Communication: Further summer speedup of Jakobshavn Isbræ." The Cryosphere 8: 209–214. doi:10.5194/tc-8-209-2014.

Keegan, K. M., R.M. Albert, J. R. McConnell and I. Baker. 2014. "Climate change and forest fires synergistically drive widespread melt events of the Greenland Ice Sheet." Proceedings of the National Academy of Sciences 111(22): 7964–7967. doi: 10.1073/pnas.1405397111.

Khan, S. A., L. Liu, J. Wahr, I. Howat, I. Joughin, T. van Dam, and K. Fleming. 2010. "GPS measurements of crustal uplift near Jakobshavn Isbræ due to glacial ice mass loss." Journal of Geophysical Research 115: B09405. doi:10.1029/2010JB007490.

Khan, S. A., K. H. Kjær, M. Bevis, J. L. Bamber, J. Wahr, K. K. Kjeldsen, A. A. Bjørk, N. J. Korsgaard, L. A. Stearns, M. R. van den Broeke, L. Liu, N. K. Larsen, and I. S. Muresan. 2014. "Sustained Mass Loss of the Northeast Greenland Ice Sheet Triggered by Regional Warming." Nature Climate Change 4: 292–299. doi:10.1038/nclimate2161.

Khan, S. A., A. Aschwanden, A. A. Bjørk, J. Wahr, K. K. Kjeldsen, and K. H. Kjær. 2015. "Greenland ice sheet mass balance: a review." Reports on Progress in Physics 78(4). doi: 10.1088/0034-4885/78/4/046801.

Kimura, S., P. R. Holland, A. Jenkins, and M. Piggott. 2014. "The effect of meltwater plumes on the melting of a vertical glacier face." Journal of Physical Oceanography 44: 3099-3117. doi: 10.1175/JPO-D-13-0219.1

Krabill, W., W. Abdalati, E. Frederick, S. Manizade, C. Martin, J. Sonntag, R. Swift, R. Thomas, W. Wright, and J. Yungel. 2000. "Greenland Ice Sheet: High-Elevation Balance and Peripheral Thinning." Science 289: 428–430. doi:10.1126/science.289.5478.428.

Krabill, W., E. Hanna, P. Huybrechts, W. Abdalati, J. Cappelen,B. Csatho, E. Frederick, S. Manizade, C. Martin, J. Sonntag,R. Swift, R. Thomas, and J. Yungel. 2004. "Greenland Ice Sheet: Increased coastal thinning", Geophysical Research Letters 31: L24402. doi:10.1029/2004GL021533.

Krabill, W. B. 2014. “IceBridge ATM L2 Icessn Elevation, Slope, and Roughness, [1993-2014]. Boulder, Colorado USA: NASA Distributed Active Archive Center at the National Snow and Ice Data Center. Digital media.Updated 2014.” http://nsidc.org/data/ilatm2.html.

Larour, E., H. Seroussi, M. Morlighem, and E. Rignot. 2012. “Continental scale, high order, high spatial resolution, ice sheet modeling using the Ice Sheet System Model (ISSM).” Journal of Geophysical Research: Earth Surface (2003-2012) 117: F01022. doi:10.1029/2011JF002140.

Levermann, A., T. Albrecht, R. Winkelmann, M. A. Martin, M. Haseloff, and I. Joughin. 2012. “Kinematic first-order calving law implies potential for abrupt ice-shelf retreat.” The Cryosphere 6: 273–286. doi:10.5194/tc-6-273-2012.

Luckman, A., and T. Murray. 2005. “Seasonal variation in velocity before retreat of Jakobshavn Isbræ, Greenland.” Journal of Geophysical Research Letters 32: L08501. doi:10.1029/2005GL022519.

MacAyeal, D. R., T. A. Scambos, C. L. Hulbe and M. A. Fahnestock. 2003. “Catastrophic iceshelf break-up by an ice-shelf-fragment-capsize mechanism.” Journal of Glaciology 49(164): 22-36.

Martin, M. A., R. Winkelmann, M. Haseloff, T. Albrecht, E. Bueler, C. Khroulev, and A. Levermann. 2011. “The Potsdam Parallel Ice Sheet Model (PISM-PIK), Part II: Dynamical equilibrium simulation of the Antarctic Ice Sheet.” The Cryosphere 5: 727–740. doi:10.5194/tc-5-727-2011.

Mengel, M., and A. Levermann. 2014. “Ice plug prevents irreversible discharge from East Antarctica.” Nature Climate Change 4: 451–455. doi:10.1038/nclimate2226.

Moon, T., I. Joughin, B. Smith, and I. Howat. 2012. “21st-Century evolution of Greenland outlet glacier velocities.” Science 336: 576–578. doi:10.1126/science.1219985.

Motyka, R. J., M. Truffer, M. Fahnestock, J. Mortensen, S. Rysgaard, and I. Howat. 2011. “Submarine melting of the 1985 Jakobshavn Isbræ floating tongue and the triggering of the current retreat.” Journal of Geophysical Research 116: F01007. doi:10.1029/2009JF001632.

NSIDC. 2015. “2014 melt season in review.” National Snow & Ice Data Center (NSIDC). Accessed July 09, 2015. http://nsidc.org/greenland-today/2015/01/2014-melt-season-in-review/.

Nghiem, S. V., D. K. Hall, T. L. Mote, M. Tedesco, M. R. Albert, K. Keegan, C. A. Shuman, N. E. DiGirolamo, and G. Neumann. 2012. “The extreme melt across the Greenland ice sheet in 2012.” Geophysical Research Letters 39: L20502. doi: 10.1029/2012GL053611.

Nick, F. M., A. Vieli, M. L. Andersen, I. Joughin, A. Payne, T. L. Edwards, F. Pattyn, and R. S. van de Wal. 2013. “Future sea-level rise from Greenland’s main outlet glaciers in a warming climate.” Nature 497: 235–238. doi:10.1038/nature12068.

Nick, F.M., A. Vieli, I. M. Howat, and I. Joughin. 2009. “Large-Scale Changes in Greenland Outlet Glacier Dynamics Triggered at the Terminus.” Nature Geoscience 2: 110–114. doi:10.1038/ngeo394.

Nielsen, K., S. A. Khan, G. Spada, J. Wahr, M. Bevis, L. Liu, and T. van Dam. 2013. “Vertical and horizontal surface displacements near Jakobshavn Isbræ driven by melt-induced and dynamic ice loss.” Journal of Geophysical Research Solid Earth 118: 1837–1844. doi:10.1002/jgrb.50145.

Noël, B., W. J. van de Berg, E. van Meijgaard, P. Kuipers Munneke, R. S. W. van de Wal, and M. R. van den Broeke. 2015. “Summer snowfall on the Greenland Ice Sheet: a study with the updated regional climate model RACMO2.3.” The Cryosphere Discussion 9: 1177-1208. doi: 10.5194/tcd-9-1177-2015.

Parizek, B.R., and R.T. Walker. 2010. “Implications of initial conditions and ice–ocean coupling for grounding-line evolution.” Earth and Planetary Science Letters 300: 351–358. doi:10.1016/j.epsl.2010.10.016.

Pattyn, F., C. Schoof, L. Perichon, R. C. A. Hindmarsh, E. Bueler, B. de Fleurian, G. Durand, et al. 2012. “Results of the Marine Ice Sheet Model Intercomparison Project, MISMIP.” The Cryosphere 6: 573–588. doi:10.5194/tc-6-573-2012.

Pollard, D., R. M. DeConto, and R. B. Alley. 2015. “Potential Antarctic Ice Sheet retreat driven by hydrofracturing and ice cliff failure.” Earth and Planetary Science Letters 412: 112–121. doi: 10.1016/j.epsl.2014.12.035.

Price, S. F., A. J. Payne, I. M. Howat, and B. E. Smith. 2011. “Committed sea-level rise for the next century from Greenland ice sheet dynamics during the past decade.” Proceedings of the National Academy of Sciences of the United States of America 108: 8978–8983. doi:10.1073/pnas.1017313108.

Rignot, E., J. L. Bamber, M. R. van den Broeke, C. Davis, Y. Li, W. J. van de Berg, and E. van Meijgaard. 2008. "Recent Antarctic ice mass loss from radar interferometry and regional climate modeling." Nature Geoscience 1: 106–110. doi:10.1038/ngeo102.

Schoof, C. 2007. "Ice sheet grounding line dynamics: steady states, stability, and hysteresis." Journal of Geophysical Research 112 (F03S28). doi:10.1029/2006JF000664.

Seroussi, H., H. B. Dhia, M. Morlighem, E. Larour, E. Rignot, and D. Aubry. 2012. "Coupling ice flow models of varying orders of complexity with the Tiling method." Journal of Glaciology 58: 776–786. doi:10.3189/2012JoG11J195.

Shapiro, N. M., and M. H. Ritzwoller. 2004. "Inferring surface heat flux distributions guided by a global seismic model: particular application to Antarctica." Earth and Planetary Science Letters 223: 213–224. doi: 10.1016/j.epsl.2004.04.011.

Shepherd, A., E. R. Ivins, A. Geruo, V. R. Barletta, M. J. Bentley, S. Bettadpur, K. H. Briggs, D. H. Bromwich, et al. 2012. "A reconciled estimate of ice-sheet mass balance." Science 338(6111): 1183-1189. doi:10.1126/science.1228102.

Slater, D. A., P. W. Nienow, T. R. Cowton, D. N. Goldberg, and A. J. Sole. 2015. "Effect of near-terminus subglacial hydrology on tidewater glacier submarine melt rates." Geophysical Research Letters 42: 2861-2868. doi: 10.1002/2014GL062494.

Stanley, S. J., A. Jenkins, C. F. Giulivi and P. Dutrieux. 2011. "Stronger ocean circulation and increased melting under Pine Island Glacier ice shelf." Nature Geoscience 4: 519–523. doi: 10.1038/ngeo1188

Tedesco, M., X. Fettweis, T. Mote, J. Wahr, P. Alexander, J. E. Box, and B. Wouters. 2013. "Evidence and analysis of 2012 Greenland records from spaceborne observations, a regional climate model and reanalysis data." The Cryosphere 7: 615-630. doi: 10.5194/tc-7-615-2013

The PISM Authors. 2014. "PISM, a Parallel Ice Sheet Model. User's Manual." Accessed June 15, 2015. http://www.pism-docs.org/wiki/lib/exe/fetch.php?media=manual.pdf.

Thomas, H. R., W. Abdalati, E. Frederick, W. B. Krabill, S. Manizade, and K. Steffen. 2003. "Investigation of surface melting and dynamic thinning on Jakobshavn Isbræ." Journal of Glaciology 49 (165): 231–239. doi:10.3189/172756503781830764.

Thomas, R. H. 2004. “Force-perturbation analysis of recent thinning and acceleration of Jakobshavn Isbrae, Greenland.” Journal of Glaciology 50(168): 57–66. doi: 10.3189/172756504781830321.

Van der Veen, C. J., J. C. Plummer, and L. A. Stearns. 2011. “Controls on the recent speed-up of Jakobshavn Isbræ, West Greenland.” Journal of Glaciology 57 (204): 770–782.

Vieli, A., and F. M. Nick. 2011. “Understanding and Modeling Rapid Dynamic Changes of Tidewater Outlet Glaciers: Issues and Implications.” Surveys in Geophysics 32: 437–458. doi: 10.1007/s10712-011-9132-4.

Winkelmann, R., M. A. Martin, M. Haseloff, T. Albrecht, E. Bueler, C. Khroulev, and A. Levermann. 2011. “The Potsdam Parallel Ice Sheet Model (PISM-PIK) Part 1: Model description.” The Cryosphere 5: 715–726. doi:10.5194/tc-5-715-2011.

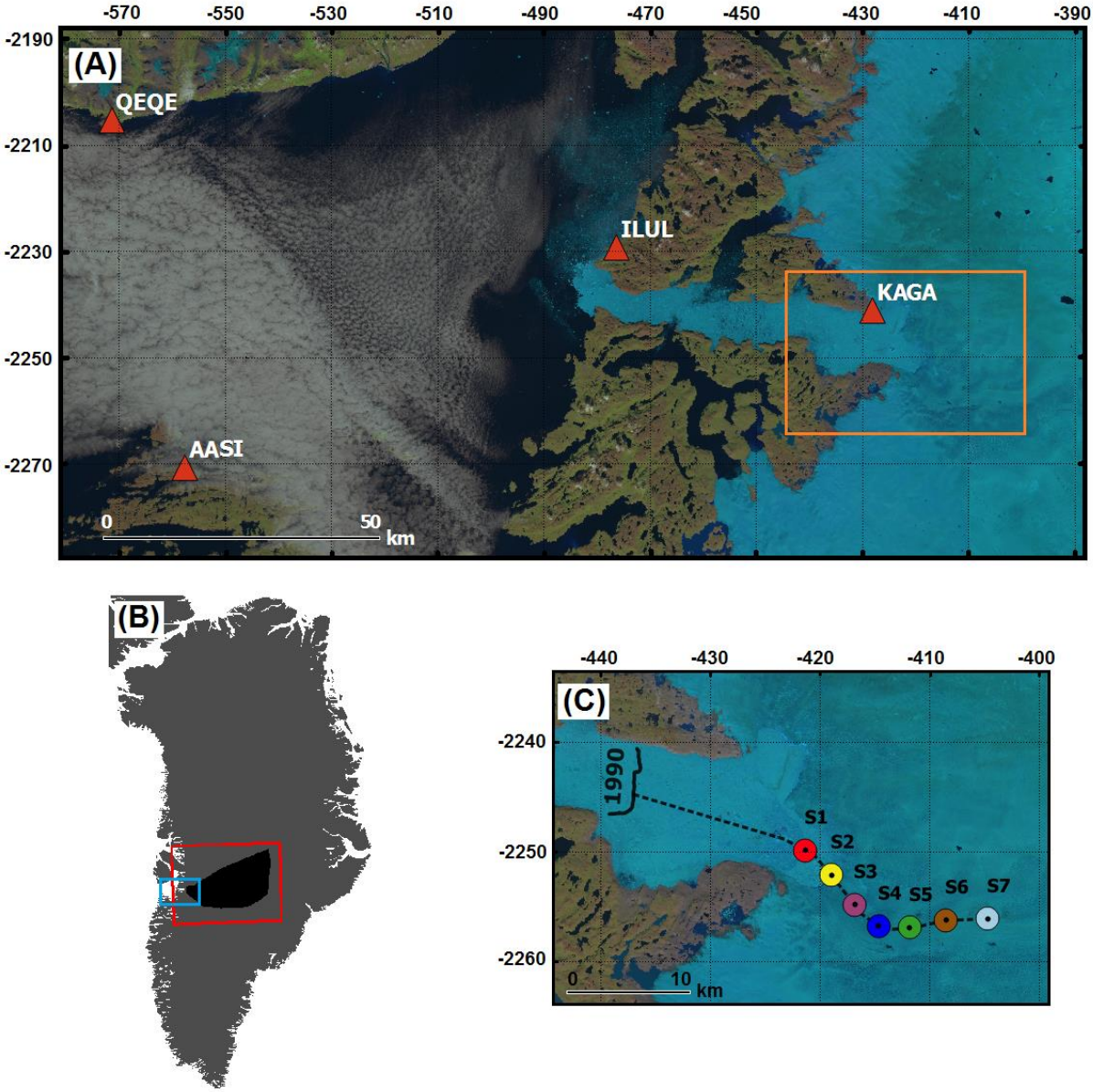

Figure 1. (A) Landsat 8 image of Ilulissat fjord and part of Disko Bay acquired in August 2014. The dark orange triangles indicate the locations of the GPS stations (GPS data shown in Fig. 5). The polygon defined by light orange borders outlines the location of Fig. 1C. (B) Grey filled Greenland map. The black filled polygon highlights the JI basin used to compute the mass loss (Fig. 4) and is identical to Khan et al. 2014. The polygon defined by red borders indicates the computational domain. The light blue border polygon represents the location of Fig. 1A. (C) Coloured circles indicate the locations plotted in Fig. 3. The thick black line denotes the JI terminus position in the 1990s. The dotted black line represents the flow-line location plotted in Fig. 6. The coordinates given in (A) and (C) are in polar-stereographic projection units (km).

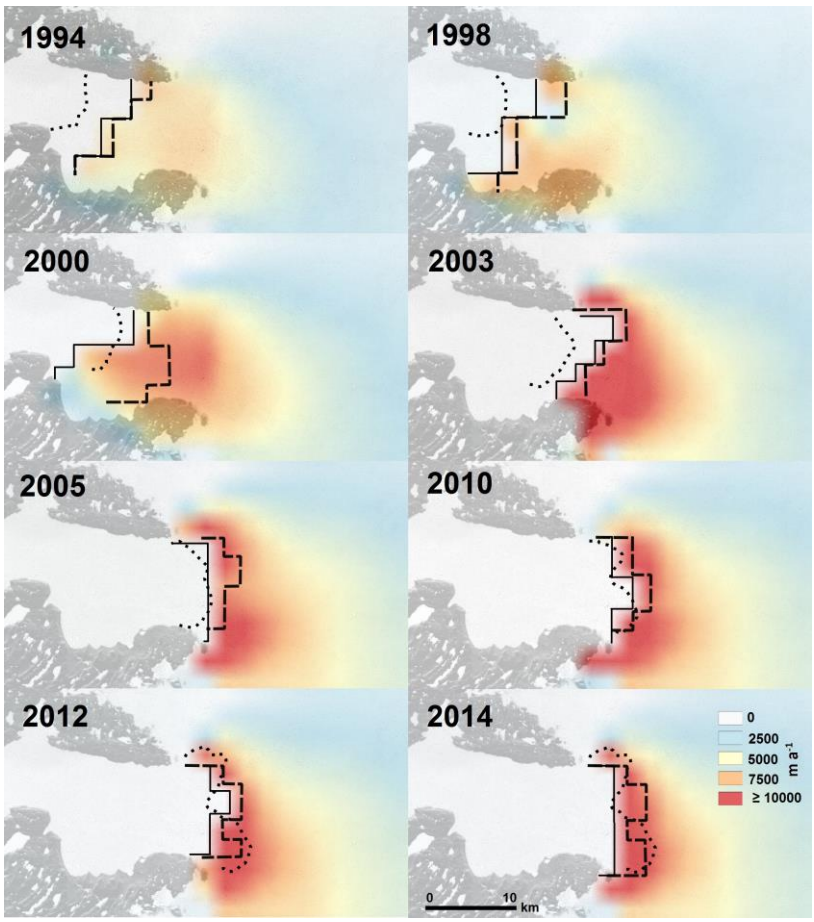

Figure 2. Modelled velocities at Jakobshavn Isbræ for December are shown for seven different years. The black line represents the modelled front positions, the black dotted line denotes the observed front position and the thick black dashed line represents the modelled grounding line position. The velocities are superimposed over a Landsat 8 image acquired in August 2014.

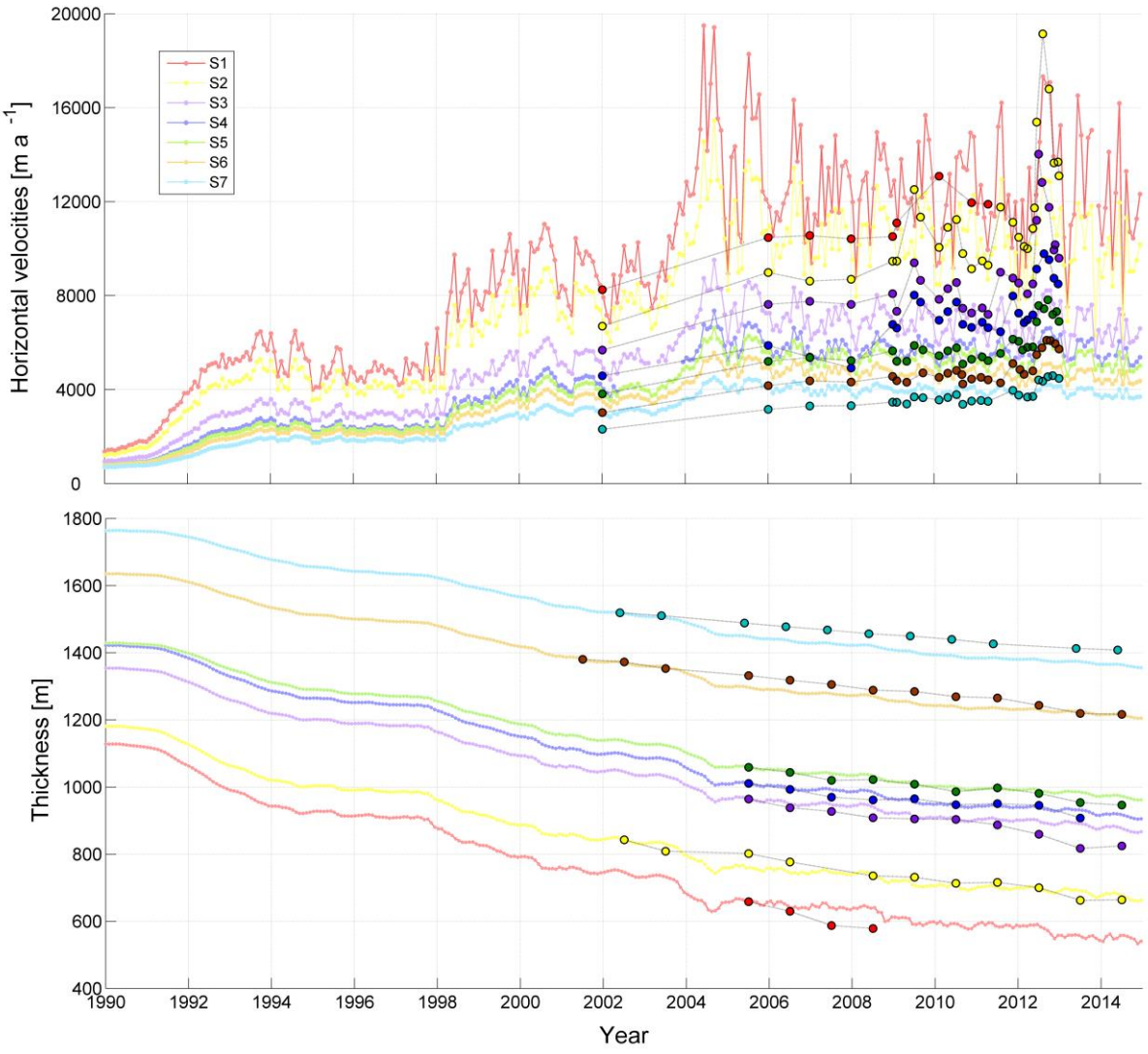

Figure 3. (A) Time series of modelled (filled circles) versus observed (filled circles with black edges) velocities (Joughin et al., 2010) (top figure) and ice thickness changes (Krabill, 2014) (bottom figure) for the period 1990-2014 at locations (S1 to S7) shown in Fig. 1C. The same colour scheme is used for the modelled and the observed data. The observed thickness has been adjusted to match the model thickness at the first year.

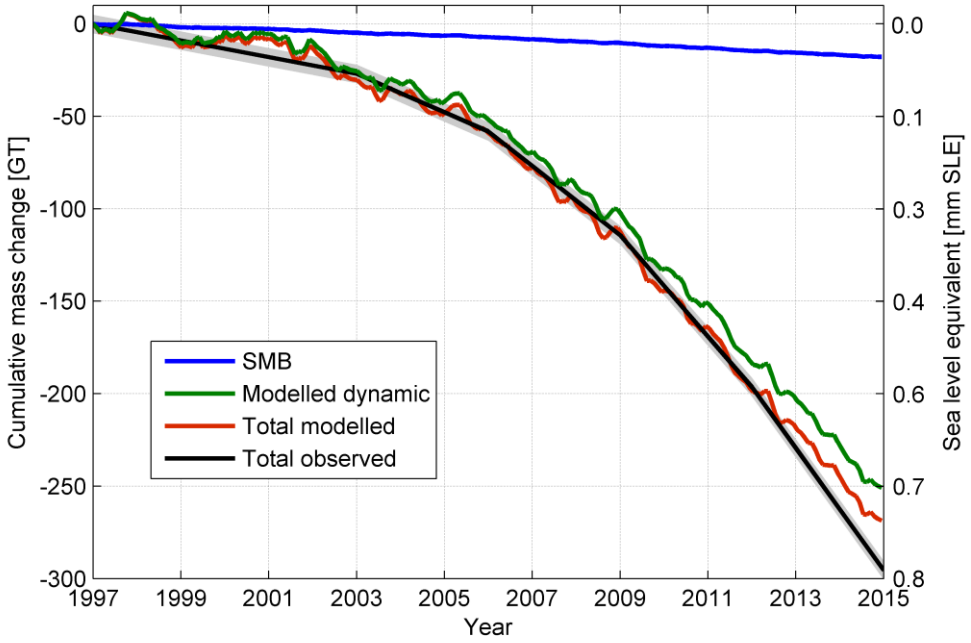

Figure 4. Modelled and observed cumulative mass change for Jakobshavn Isbræ. The blue curve represents the mass change due to SMB after the 1960-1990 baseline is removed. The green curve represents the modelled ice dynamics mass change. To estimate the mass change due to changes in ice dynamics, we subtract the SMB mass change (as calculated based on RACMO 2.3 (Noël et al., 2015)) from the total modelled mass change. The red curve represents the total modelled mass change including both SMB and ice dynamic changes. The black curve with grey error limits represents the total observed mass change including both SMB and ice dynamic changes. The modelled mass change for the period 1997-2014 is ~269 Gt and the observed mass change is ~296 Gt.

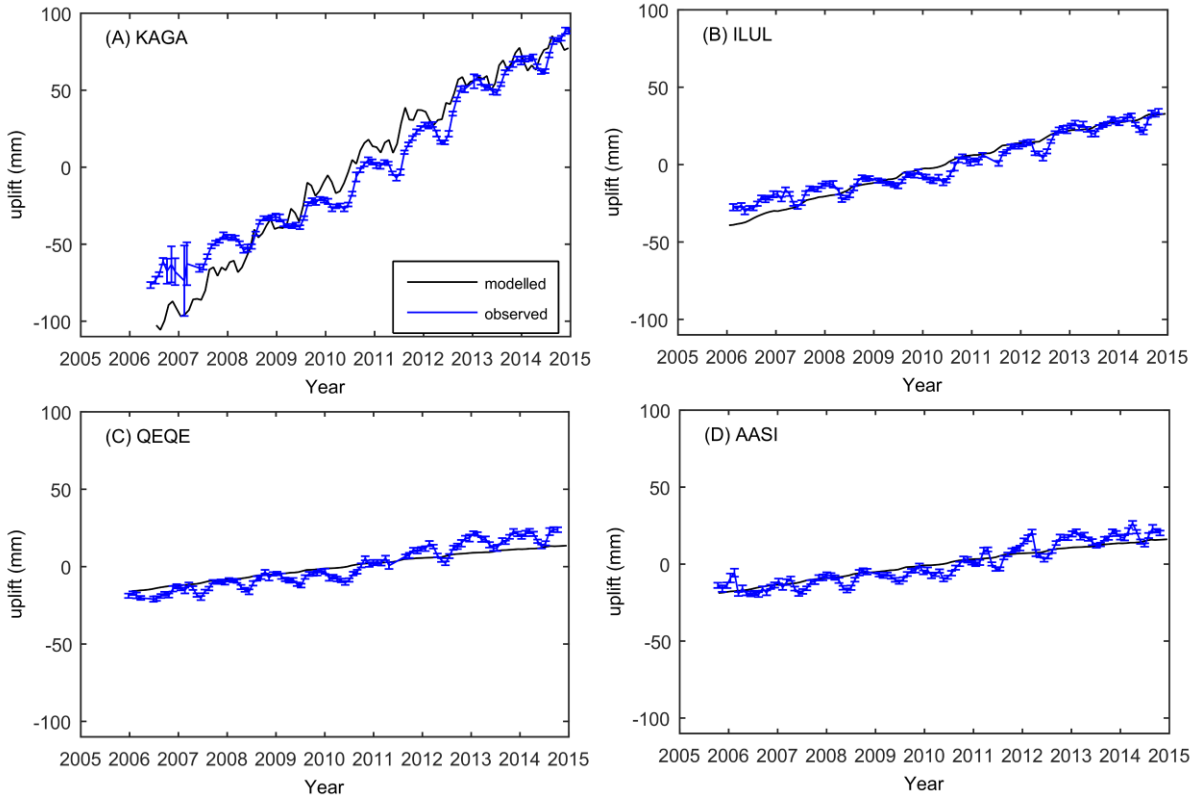

Figure 5. Observed versus modelled uplift in mm for the stations KAGA (A), ILUL (B), QEQE (C) and AASI (D). The positions of the four GPS stations are presented in Fig. 1A.

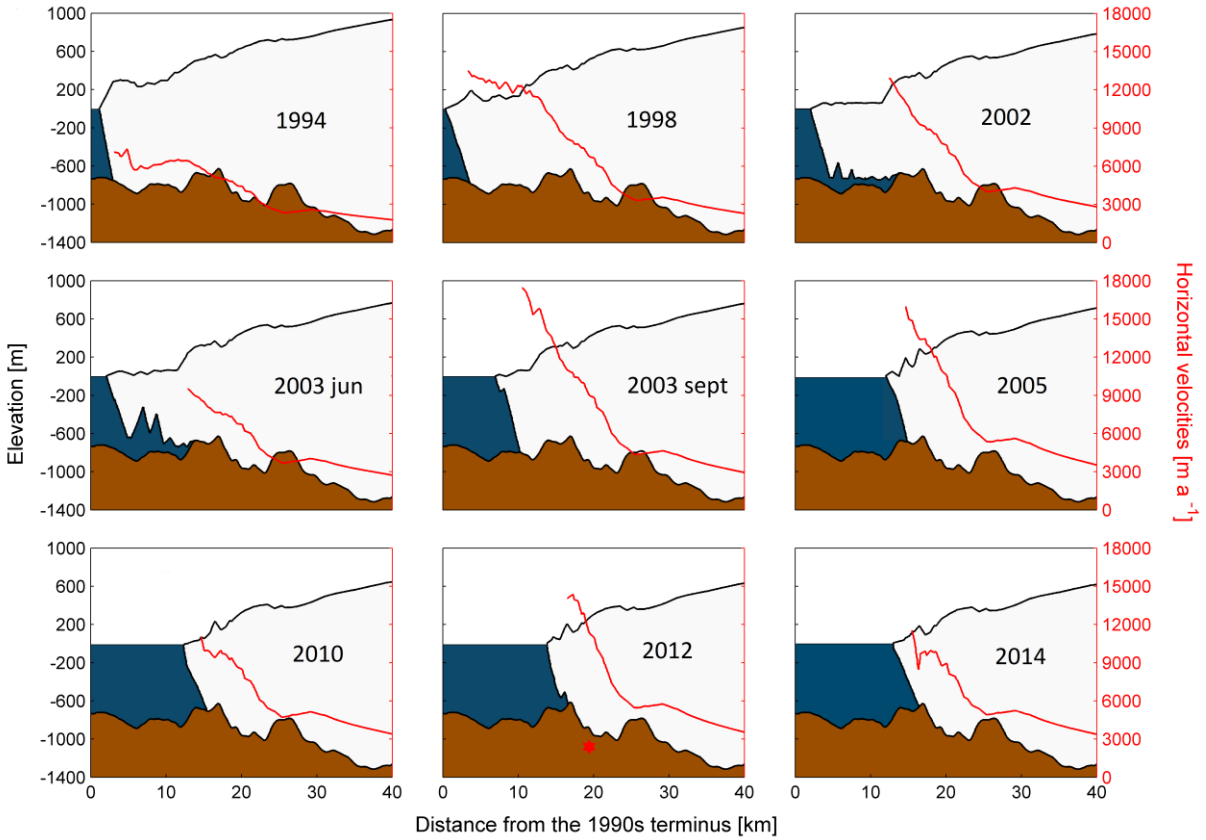

Figure 6. Modelled evolution of surface elevation (ice shelves thinner than 50 m are not shown) and horizontal velocities of Jakobshavn Isbræ for December along the flow-line shown in Fig. 1C. Note the acceleration in speed between 1994-1998 and between June 2003 and September 2003 corresponding to the final breakup of the floating tongue. The red star denotes the observed 2012 terminus position.